552 *Inorg. Chem.* **2010**, *49*, 552–560
DOI: 10.1021/ic901571m

Inorganic Chemistry
Article

Covalent Bonding and the Trans Influence in Lanthanide Compounds

Karsten Krogh-Jespersen,* Michael D. Romanelli, Jonathan H. Melman, Thomas J. Emge, and John G. Brennan*

Department of Chemistry and Chemical Biology, Rutgers, The State University of New Jersey, New Brunswick, New Jersey 08903

Received August 14, 2009

A pair of *mer*-octahedral lanthanide chalcogenolate coordination complexes $[(THF)_3Ln(EC_6F_5)_3$ (Ln = Er, E = Se; Ln = Yb, E = S)] have been isolated and structurally characterized. Both compounds show geometry-dependent bond lengths, with the Ln−E bonds trans to the neutral donor tetrahydrofuran (THF) significantly shorter than the Ln−E bonds that are trans to negatively charged EC_6F_5 ligands. Density functional theory calculations indicate that the structural trans influence evidenced by the differences in these bond lengths results from a covalent Ln−E interaction involving ligand p and Ln 5d orbitals.

Introduction

A fundamental understanding of f-block chemistry remains a seminal challenge, thwarted by the complex angular properties of the f orbitals and the varying relative extensions of (n)f vs $(n+1)$d and $(n+2)$s,p orbitals. Molecular actinide chemistry has examples of clearly defined covalent bonding interactions involving overlap with 5f orbitals, as illustrated in the coordination of carbon monoxide to uranium(III)[1,2] or the variable-energy photoelectron spectra of uranocene.[3] Numerous structural pairs[4−7] exist for which actinide−ligand bond lengths do not obey the simple radius summation rules[8,9] that for decades dominated the interpretation of bond lengths in actinide complexes.

In contrast, structure/property relationships in lanthanide (Ln) chemistry have always appeared to be less complicated. Ln magnetic properties can almost always be treated as classical isolated spin systems, with 4f−4f interactions rarely measurable above 20 K. Ln electronic properties are also notoriously independent of the coordination sphere, to the extent that the electronic spectra of solid-state ErF_3 and molecular $(DME)_2Er(SC_6F_5)_3$ are virtually identical.[10] Structural features, until recently, could always be rationalized by ionic bonding models, with bond lengths predicted by the summation of ionic radii, taking into account the metal oxidation state and coordination number. In the past decade, however, exceptions to these rules have appeared.

In transition-metal and main-group chemistry, covalent bonding interactions often produce a trans effect, in which a metal−ligand bond length has been influenced by the identity of the ligand trans to the bond in question.[11] We originally noted years ago, in the description of the *mer*-octahedral lanthanide thiolate coordination compound $(py)_3Yb(SPh)_3$,[12] that there appeared to be a structural trans influence, with the Yb−S bond trans to SPh being significantly longer than the Yb−S bond trans to the neutral pyridine donor. The same nonclassical bond-length distributions have since been observed in a series of related compounds, including chalcogenido clusters[13,14] and, most recently, a fluorinated phenolate.[15]

*To whom correspondence should be addressed. E-mail: kroghjes@rci.rutgers.edu (K.K.-J.), bren@rci.rutgers.edu (J.G.B.).

(1) (a) Parry, J.; Carmona, E.; Coles, S.; Hursthouse, M. *J. Am. Chem. Soc*. **1995**, *117*, 2649. (b) Brennan, J. G.; Andersen, R. A.; Robbins, J. L. *J. Am. Chem. Soc*. **1986**, *108*, 335.
(2) Evans, W. J.; Kozimor, S. A.; Nyce, G. W.; Ziller, J. W. *J. Am. Chem. Soc*. **2003**, *125*, 12821.
(3) Brennan, J. G.; Cooper, G.; Green, J. C.; Payne, M. P.; Redfern, C. M. *J. Am. Chem. Soc*. **1989**, *111*, 2373.
(4) Brennan, J. G.; Stults, S. D.; Andersen, R. A.; Zalkin, A. *Organometallics* **1988**, *7*, 1329.
(5) Brennan, J. G.; Stults, S. D.; Andersen, R. A.; Zalkin, A. *Inorg. Chim. Acta* **1987**, *139*, 201.
(6) Mehdoui, T.; Berthet, J. C.; Thuery, P.; Ephritikhine, M. *Dalton Trans*. **2004**, 579.
(7) Mazzanti, M.; Wietzke, R. L.; Pecaut, J.; Latour, J. M.; Maldivi, P.; Remy, M. *Inorg. Chem*. **2002**, *41*, 2389.
(8) Raymond, K. N.; Eigenbrot, C. W. *Acc. Chem. Res*. **1980**, *13*, 276.
(9) Shannon, R. D. *Acta Crystallogr., Sect. A* **1976**, *32*, 751.
(10) Kornienko, A.; Emge, T. J.; Kumar, G. A.; Riman, R. E.; Brennan, J. G. *J. Am. Chem. Soc*. **2005**, *127*, 3501.
(11) (a) Appleton, T. G.; Clark, H. C.; Manzer, L. E. *Coord. Chem. Rev*. **1973**, *10*, 335. (b) Nakajima, K.; Kojima, M.; Fujita, J.; Ishii, T.; Ohba, S.; Ito, M.; Saito, Y. *Inorg. Chim. Acta* **1985**, *99*, 143. (c) Roecker, L.; Dickman, M. H.; Nosco, D. L.; Doedens, R. J.; Deutsch, E. *Inorg. Chem*. **1983**, *22*, 2022. (d) Kastner, M. E.; Smith, D. A.; Kuzmission, A. G.; Cooper, J. N.; Tyree, T.; Yearick, M. *Inorg. Chim. Acta* **1989**, *158*, 185. (e) Elder, R. C.; Trkula, M. *Inorg. Chem*. **1977**, *16*, 1048. (f) Stein, C. A.; Ellis, P. E., Jr.; Elder, R. C.; Deutsch, E. *Inorg. Chem*. **1976**, *15*, 1618. (g) Elder, R. C.; Trkula, M. *J. Am. Chem. Soc*. **1974**, *96*, 2635.
(12) Lee, J.; Brewer, M.; Berardini, M.; Brennan, J. *Inorg. Chem*. **1995**, *34*, 3215.
(13) Freedman, D.; Melman, J. H.; Emge, T. J.; Brennan, J. G. *Inorg. Chem*. **1998**, *37*, 4162.
(14) Kornienko, A.; Emge, T.; Hall, G.; Brennan, J. G. *Inorg. Chem*. **2002**, *41*, 121.
(15) Norton, K.; Kumar, G. A.; Dilks, J. L.; Emge, T. J.; Riman, R. E.; Brik, M. G.; Brennan, J. G. *Inorg. Chem*. **2009**, *48*, 3573.

 Published on Web 12/21/2009

Trans influences have also been noted in pairs of chemically related compounds,[16] but interpretations of the different bond lengths are complicated by the difficulty of comparing compounds for which different steric properties or different crystal-packing forces may also be influencing the length of the Ln−ligand bond.

While theoretical descriptions of covalent actinide−ligand bonding abound, i.e., $U(C_8H_8)_2$[17,18] or $Cp_3U(L)$ (L = CO, PR_3),[19−21] examinations of Ln systems with clearly defined covalent characteristics have yet to reveal any physical characteristics that could clearly be attributed to a degree of covalent bonding. The bis-arene lanthanides have been described[22−24] in terms of significant M−L π donation between the Ln d orbitals and the arene π^* orbitals. A density functional theory (DFT) analysis of eight-coordinate Ln compounds with S-based anions concluded that Ln−S bonds are, in fact, "ionocovalent", but a clear illustration of how covalent bonding might impact the physical properties could not be discerned, given the difficulty of visualizing orbital overlap in these eight-coordinate structures.[25] Finally, a theoretical investigation into the bonding in $Ln(N(ER)_2)_3$ suggested that the Ln−E bonds were essentially ionic in either the octahedral (all E) or nine-coordinate (6E, 3N) geometries.[26] The coordination environments in all of these Ln compounds were either too symmetric or too asymmetric to reveal any directional bonding effects.

Because Ln ions are extensively used in catalysis, an appreciation of the extent to which covalent bonding might impact Ln systems is of practical importance, and the development of proper methodologies for computational modeling of such processes is highly advantageous. Here we outline the synthesis and structural characterization of two new *mer*-octahedral Ln coordination complexes with S- and Se-based anions, and we present results from DFT calculations that suggest that the observed bond-length distributions originate from covalent bonding involving the overlap of ligand-based p orbitals with the Ln 5d orbitals.

Experimental Section

General Methods. All syntheses were carried out under ultrapure nitrogen (Welco Praxair), using conventional drybox or Schlenk techniques. Tetrahydrofuran (THF; Aldrich) was purified with a dual-column Solv-Tek solvent purification system and collected immediately prior to use. $Hg(SC_6F_5)_2$ was prepared according to a modified procedure[27] of the initial synthesis,[28] and $(SeC_6F_5)_2$[29] was prepared according to the literature. Er (chips) and Yb (powder) metals were purchased from Aldrich and used as received. Melting points were recorded in sealed capillaries and are uncorrected. IR spectra were recorded on a Thermo Nicolet Avatar 360 FTIR spectrometer from 4000 to 450 cm^{-1} as Nujol mulls on CsI plates. Visible absorbance spectra were recorded on either a Varian DMS 100S spectrometer or a Cary 50 Bio with the samples dissolved in THF, placed in either a 1.0 mm × 1.0 cm Spectrosil quartz cell or a 1.0 cm^2 special optical glass cuvette, and scanned between 190 and 1000 nm, with ranges depending on the metal ion present in the sample. Elemental analyses were performed by Quantitative Technologies, Inc. (Whitehouse, NJ).

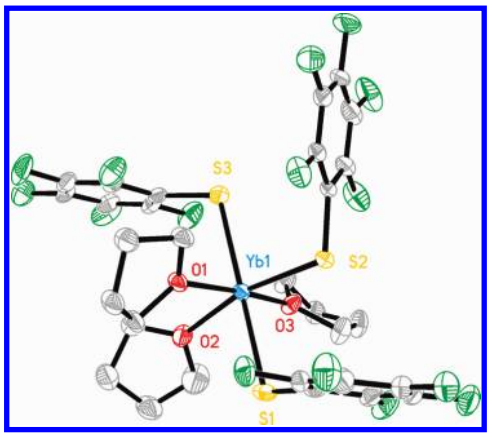

Figure 1. ORTEP diagram of **1** with green indicating F atoms and gray C atoms. The H atoms were removed for clarity.

Synthesis of $(THF)_3Yb(SC_6F_5)_3$ (1). Yb (0.083 g, 0.48 mmol) and $Hg(SC_6F_5)_2$ (0.447 g, 0.747 mmol) were combined in THF (20 mL), and the mixture was stirred until Yb was consumed and elemental Hg was visible in the bottom of the flask (overnight). The pale-yellow solution was filtered away from the Hg (0.11 g, 73%), reduced in volume under vacuum to ca. 15 mL, and layered with hexane (15 mL) to give yellow crystals (0.098 g, 21%) that melt at 79 °C, give a yellow-orange solid at 135 °C, and continue to darken up to 350 °C. IR: 2950 (s), 2855 (s), 2724 (w), 1625 (w), 1508 (s), 1462 (s), 1377 (s), 1261 (w), 1172 (w), 1074 (m), 1002 (m), 971 (m), 857 (m), 722 (w) cm^{-1}. UV−vis: For a 6.1 mM THF solution with a 1.00 cm path length, this compound shows a broad absorption maximum centered at 394 nm (ε = 208 $L\cdot mol^{-1}\cdot cm^{-1}$) and a shoulder at 486 nm (ε = 88 $L\cdot mol^{-1}\cdot cm^{-1}$). Anal. Calcd for $C_{30}H_{24}YbF_{15}O_3S_3$: C, 36.5; H, 2.45. Found: C, 36.5; H, 2.56. Single-crystal X-ray diffraction data (233 K): space group $P2_1/c$; a = 9.581(2) Å; b = 15.885(2) Å; c = 25.035(3) Å; β = 100.03(1)°; V = 3452.3(9) $Å^3$; Z = 4; D_{calcd} = 1.898 $g\cdot cm^{-3}$.

Synthesis of $(THF)_3Er(SeC_6F_5)_3$ (2). Er (0.084 g, 0.50 mmol), $(SeC_6F_5)_2$ (0.37 g, 0.75 mmol), and Hg (0.026 g) were combined in THF (ca. 20 mL), and the mixture was stirred until the metal flakes were completely consumed (8 days). The pale-pink solution was filtered and concentrated to ~5 mL. The solution was held at −5 °C for 2 days, brought to room temperature, and layered 2:1 with hexanes to give pale-pink lathes (0.42 g, ~75%) that melt at 153 °C. IR: 2958 (s), 1634 (w), 1605 (w), 1531 (w), 1507 (s), 1474 (s), 1254 (m), 1070 (s), 960 (s), 809 (s), 669 (m), 604 (w) cm^{-1}. UV−vis: For a 0.104 M THF solution with a 1.00 mm path length, this compound shows absorption maxima at 655 (2.04 $L\cdot mol^{-1}\cdot cm^{-1}$), 547 ($\varepsilon$ = 1.3 $L\cdot mol^{-1}\cdot cm^{-1}$), 523 ($\varepsilon$ = 27 $L\cdot mol^{-1}\cdot cm^{-1}$), 490 ($\varepsilon$ = 3.3 $L\cdot mol^{-1}\cdot cm^{-1}$), 453 ($\varepsilon$ = 3.0 $L\cdot mol^{-1}\cdot cm^{-1}$), 409 ($\varepsilon$ = 8.6 $L\cdot mol^{-1}\cdot cm^{-1}$), and 380 ($\varepsilon$ = 75 $L\cdot mol^{-1}\cdot cm^{-1}$) nm. These absorption peaks correspond to the $^4F_{9/2}$, $^4S_{3/2}$, $^2H_{11/2}$, $^4F_{7/2}$, $^4F_{5/2,3/2}$, $^2G_{9/2}$, and $^4G_{11/2}$

(16) (a) Deacon, G. B.; Feng, T.; Skelton, B. W.; White, A. H. *Aust. J. Chem.* **1995**, *48*, 741. (b) Panda, T. K.; Trambitas, A. G.; Bannenberg, T.; Hrib, C. G.; Randoll, S.; Jones, P. G.; Tamm, M. *Inorg. Chem* **2009**, *48*, 5462.
(17) Moritz, A.; Dolg, M. *Chem. Phys.* **2007**, *337*, 48.
(18) Rosch, N.; Streitweiser, A. *J. Am. Chem. Soc.* **1983**, *105*, 7237.
(19) Vetere, V.; Maldivi, P.; Adamo, C. *J. Comput. Chem.* **2003**, *24*, 850.
(20) Bursten, B. E.; Rhodes, L. F.; Strittmatter, R. J. *J. Am. Chem. Soc.* **1989**, *111*, 2758.
(21) Maron, L.; Eisenstein, O.; Andersen, R. A. *Organometallics* **2009**, *28*, 3629.
(22) DiBella, S.; Lanza, G.; Fragala, I. L.; Marks, T. J. *Organometallics* **1996**, *15*, 3985.
(23) Hong, G. Y.; Schautz, F.; Dolg, M. *J. Am. Chem. Soc.* **1999**, *121*, 1502.
(24) King, W. A.; DiBella, S.; Lanza, G.; Khan, K.; Duncalf, D. J.; Cloke, F. G. N.; Fragala, I. L.; Marks, T. J. *J. Am. Chem. Soc.* **1996**, *118*, 627.
(25) Roger, M.; Barros, N.; Arliguie, T.; Thuery, P.; Maron, L.; Ephritikhine, M. *J. Am. Chem. Soc.* **2006**, *128*, 8790.
(26) Gaunt, A. J.; Reilly, S. D.; Enriquez, A. E.; Scott, B. L.; Ibers, J. A.; Sekar, P.; Ingram, K. I. M.; Kaltsoyannis, N.; Neu, M. P. *Inorg. Chem.* **2008**, *47*, 29.
(27) Melman, J. H.; Emge, T. J.; Brennan, J. G. *Inorg. Chem.* **2001**, *40*, 1078.
(28) Peach, M. E. *J. Inorg. Nucl. Chem.* **1973**, *35*, 1046.
(29) Klapötke, T. M. *Eur. J. Inorg. Chem.* **1999**, 1359.

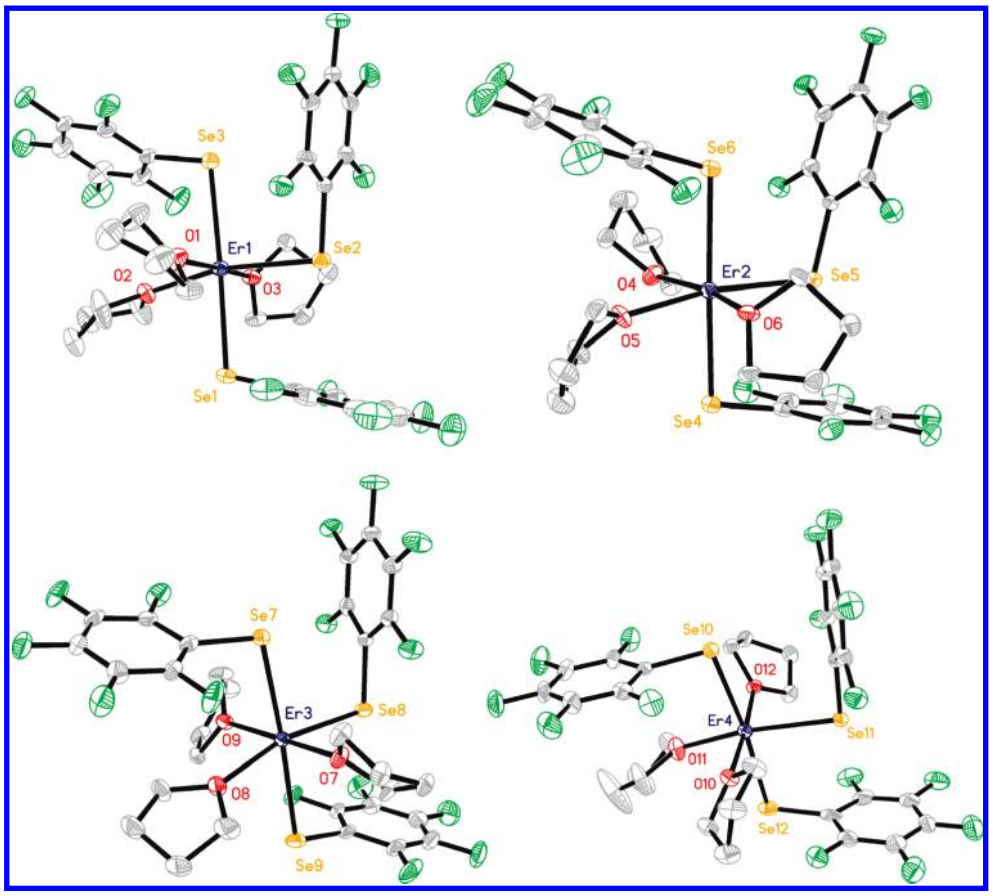

Figure 2. ORTEP diagrams for the four independent molecules within the unit cell of **2** with green indicating F atoms and gray C atoms. The H atoms were removed for clarity.

transitions typically seen from the $^4I_{15/2}$ ground state of Er^{3+}. Anal. Calcd for $C_{30}H_{24}F_{15}O_3Se_3Er$: C, 32.1; H, 2.16. Found: C, 31.6; H, 1.97. Single-crystal X-ray diffraction data (100 K): space group $P2_1$; a = 19.481(2) Å; b = 15.625(2) Å; c = 23.555(2) Å; β = 105.766(2)°; V = 6900(1) Å^3; Z = 8; D_{calcd} = 2.159 g·cm^{-3}.

X-ray Structure Determination. Data for **1** were collected on an Enraf-Nonius CAD4 diffractometer with graphite-monochromatized Mo Kα radiation (λ = 0.710 73 Å). The crystal of **1** was glued to a glass fiber and placed in a cold nitrogen stream. Data for **2** were collected on a Bruker Smart APEX CCD diffractometer with graphite-monochromatized Mo Kα radiation (λ = 0.710 73 Å) at 100 K. The crystal of **2** was immersed in Paratone oil and placed in a cold nitrogen stream. The data for **1** and **2** were corrected for Lorenz effects, polarization, and absorption, the latter by a multiscan method (*SADABS*).[30] The structures were solved by direct methods (*SHELXS86*).[31] All non-H atoms were refined (*SHELXL97*)[32] based upon F_{obs}^2. All H-atom coordinates were calculated with idealized geometries (*SHELXL97*). Scattering factors ($f°, f', f''$) are as described in *SHELXL97*. ORTEP diagrams[33] for **1** and **2** are shown in Figures 1 and 2, respectively. Significant bond lengths and angles for **1** and **2** are given in Tables 1 and 2, respectively. Complete crystallographic details are given in the Supporting Information.

Computational Details

Electronic structure calculations have been carried out at the DFT level of theory.[34] A large majority of the calculations made use of the PBE[35] combination of exchange and correlation functionals, although the TPSS,[36] B3LYP,[37] and M05[38] functionals were also tested. The SDD-model MWB57 and MWB59 quasi-relativistic effective core potentials (ECPs) were used to represent the atomic cores of the Ln atoms Er and Yb.[39] These large-core ECPs incorporate all of the electrons in the 4f shell, leaving only the $5s^25p^66s^25d^1$ (valence) electrons explicitly included in the calculations, and are appropriate for Ln^{III} oxidation states. Computational justification for the use of large-core ECPs with Ln compounds has been provided.[40] Inner-shell electrons on Se atoms were replaced by the 28-electron MWB28 ECP;[41] calculations employing BasisI (see below) also made use of an ECP for S atoms (MWB10).[41]

(30) *SADABS, Bruker Nonius area detector scaling and absorption correction*, version 2.05; Bruker-AXS Inc.: Madison, WI, **2003**.
(31) Sheldrick, G. M. *SHELXS86, Program for the Solution of Crystal Structures*; University of Göttingen: Göttingen, Germany, **1986**.
(32) Sheldrick, G. M. *SHELXL97, Program for Crystal Structure Refinement*; University of Göttingen: Göttingen, Germany, **1997**.
(33) *Persistence of Vision Raytracer*, version 3.6; **2004** [computer software retrieved from http://www.povray.org/download/].
(34) Parr, R. G.; Yang, W. *Density-Functional Theory of Atoms and Molecules*; University Press: Oxford, U.K., 1989.
(35) Perdew, J. P.; Burke, K.; Ernzerhof, M. *Phys. Rev. Lett.* **1996**, *77*, 3865.
(36) Tao, J. M.; Perdew, J. P.; Staroverov, V. N.; Scuseria, G. E. *Phys. Rev. Lett.* **2003**, *91*, 146401.
(37) (a) Becke, A. D. *J. Chem. Phys.* **1993**, *98*, 5468. (b) Lee, C.; Yang, W.; Parr, R. G. *Phys. Rev. B* **1988**, *37*, 785.
(38) Zhao, Y.; Schultz, N. E.; Truhlar, D. G. *J. Chem. Phys.* **2005**, *123*, 161103.
(39) (a) Dolg, M.; Stoll, H.; Savin, A.; Preuss, H. *Theor. Chim. Acta* **1989**, *75*, 173. (b) Dolg, M.; Stoll, H.; Preuss, H. *Theor. Chim. Acta* **1993**, *85*, 441. (c) Yang, J.; Dolg, M. *Theor. Chem. Acc.* **2005**, *113*, 212.
(40) (a) Eisenstein, O.; Maron, L. *J. Organomet. Chem.* **2002**, *647*, 190. (b) Maron, L.; Eisenstein, O. *New J. Chem.* **2001**, *25*, 255. (c) Maron, L.; Eisenstein, O. *J. Phys. Chem. A* **2000**, *104*, 7140.
(41) Bergner, A.; Dolg, M.; Kuechle, W.; Stoll, H.; Preuss, H. *Mol. Phys.* **1993**, *80*, 1431.

Table 1. Significant Bond Lengths [Å] and Angles [deg] for **1**

Yb1−O1	2.271(4)	Yb1−O3	2.280(4)
Yb1−O2	2.308(5)	Yb1−S2	2.642(2)
Yb1−S1	2.678(2)	Yb1−S3	2.680(2)
S1−C1	1.766(7)	S2−C7	1.741(6)
S3−C13	1.755(7)		
O1−Yb1−O3	172.04(16)	O1−Yb1−O2	89.74(17)
O3−Yb1−O2	82.44(17)	O1−Yb1−S2	94.51(11)
O3−Yb1−S2	93.45(13)	O2−Yb1−S2	167.45(14)
O1−Yb1−S1	90.75(12)	O3−Yb1−S1	89.64(12)
O2−Yb1−S1	81.89(14)	S2−Yb1−S1	86.25(6)
O1−Yb1−S3	87.56(12)	O3−Yb1−S3	92.21(12)
O2−Yb1−S3	99.33(14)	S2−Yb1−S3	92.65(6)
S1−Yb1−S3	177.90(6)	C1−S1−Yb1	107.2(2)
C7−S2−Yb1	108.2(2)	C13−S3−Yb1	109.1(2)

Two collections of atomic basis sets were assembled. A large number of exploratory calculations were carried out on **1**, **2**, and related species with basis sets of modest size (BasisI). BasisI consists of the small valence basis sets provided with the MWB ECPs: [5s4p3d] for Yb and Er and [2s3p] for S and Se.[39,41] In addition, S and Se atoms received a single set of d-type polarization functions.[42] The outermost p function in the [2s3p] S and Se valence basis sets effectively serves as a diffuse function. O atoms carried a Dunning−Huzinaga [3s,2p] basis set, augmented by a set of d-type polarization functions and a set of diffuse p functions,[43] whereas valence double-ζ-quality Dunning−Huzinaga basis sets were placed on all C, F, and H atoms ([3s,2p] for C and F and [2s] for H).[43] Selected calculations were made with modified Er or Yb basis sets as described in the text.

A much larger basis set, BasisII, was formed for the final calculations. BasisII contains for Er and Yb the recently developed MWB-II [6s5p5d2f2g] basis sets, which include several sets of polarization functions;[44a,b] for the Se valence electrons, we used an augmented triple-ζ-quality basis set [4s4p3d2f].[44c] All-electron Dunning-type basis sets were used for the remaining atoms: aug-cc-pVTZ for O and S atoms, D95(d) for C and F atoms, and [2s] for H atoms.[43,45] Calculations on the molecular compounds **1** and **2** involved about 600 (BasisI) and 1100 (BasisII) basis functions, respectively.

Molecular geometries were fully optimized on the potential energy surfaces. Normal-mode analysis (PBE/BasisI) verified that the located stationary points were actual minima on the PES. Electronic population analysis employed the natural bond order (NBO) scheme of Weinhold et al.[46]

All computational work was performed using the *Gaussian 03*[47] software package.

Results

mer-Octahedral coordination compounds $(THF)_3Ln(EC_6F_5)_2$ [Ln = Yb, E = S (**1**); Ln = Er, E = Se (**2**)] were isolated in high yield and fully characterized. The thiolate compound **1** is prepared most readily by

Table 2. Significant Bond Lengths [Å] and Angles [deg] for **2**

Molecule 1			
Er1−O3	2.297(4)	Er1−O1	2.304(4)
Er1−O2	2.319(4)	Er1−Se2	2.8042(7)
Er1−Se1	2.8299(7)	Er1−Se3	2.8550(7)
Se1−C1	1.915(6)	Se2−C7	1.927(6)
Se3−C13	1.906(6)		
O3−Er1−O2	85.39(14)	O3−Er1−O1	172.89(15)
O3−Er1−Se2	90.59(10)	O1−Er1−O2	87.66(16)
O2−Er1−Se2	167.16(11)	O1−Er1−Se2	96.52(12)
O1−Er1−Se1	89.27(12)	O3−Er1−Se1	91.02(10)
Se2−Er1−Se1	87.916(19)	O2−Er1−Se1	79.98(11)
O1−Er1−Se3	83.68(12)	O3−Er1−Se3	96.14(10)
Se2−Er1−Se3	91.511(19)	O2−Er1−Se3	101.04(11)
C1−Se1−Er1	105.55(17)	Se1−Er1−Se3	172.82(2)
C13−Se3−Er1	101.51(17)	C7−Se2−Er1	99.30(16)
Molecule 2			
Er2−O6	2.286(4)	Er2−O4	2.298(4)
Er2−O5	2.314(4)	Er2−Se5	2.8111(6)
Er2−Se6	2.8438(6)	Er2−Se4	2.8454(6)
Se4−C31	1.915(6)	Se5−C37	1.912(5)
Se6−C43	1.917(6)		
O6−Er2−O5	82.62(14)	O6−Er2−O4	165.27(14)
O6−Er2−Se5	94.40(10)	O4−Er2−O5	82.67(14)
O5−Er2−Se5	170.61(11)	O4−Er2−Se5	100.22(10)
O4−Er2−Se6	86.76(10)	O6−Er2−Se6	95.72(10)
Se5−Er2−Se6	87.417(18)	O5−Er2−Se6	101.71(10)
O4−Er2−Se4	85.72(10)	O6−Er2−Se4	93.49(10)
Se5−Er2−Se4	86.397(19)	O5−Er2−Se4	84.91(10)
C31−Se4−Er2	103.65(16)	Se6−Er2−Se4	169.27(2)
C43−Se6−Er2	104.13(17)	C37−Se5−Er2	104.71(16)
Molecule 3			
Er3−O7	2.314(4)	Er3−O9	2.318(4)
Er3−O8	2.322(4)	Er3−Se8	2.8042(6)
Er3−Se9	2.8233(7)	Er3−Se7	2.8278(6)
Se7−C61	1.919(6)	Se8−C67	1.917(5)
Se9−C73	1.894(7)		
O7−Er3−O8	85.91(14)	O7−Er3−O9	175.50(14)
O7−Er3−Se8	91.06(10)	O9−Er3−O8	90.56(14)
O8−Er3−Se8	166.48(11)	O9−Er3−Se8	93.01(10)
O9−Er3−Se9	92.86(10)	O7−Er3−Se9	89.13(10)
Se8−Er3−Se9	89.05(2)	O8−Er3−Se9	77.74(11)
O9−Er3−Se7	88.24(10)	O7−Er3−Se7	89.43(10)
Se8−Er3−Se7	95.939(18)	O8−Er3−Se7	97.20(11)
C61−Se7−Er3	102.30(17)	Se9−Er3−Se7	174.83(2)
C73−Se9−Er3	103.37(17)	C67−Se8−Er3	99.03(16)
Molecule 4			
Er4−O12	2.304(4)	Er4−O10	2.310(4)
Er4−O11	2.337(4)	Er4−Se11	2.8019(6)
Er4−Se12	2.8276(6)	Er4−Se10	2.8334(6)
Se10−C91	1.903(5)	Se11−C97	1.913(5)
Se12−C103	1.903(7)		
O12−Er4−O11	82.62(14)	O12−Er4−O10	176.04(14)
O12−Er4−Se11	90.76(10)	O10−Er4−O11	94.91(14)
O11−Er4−Se11	165.42(10)	O10−Er4−Se11	92.34(10)
O10−Er4−Se12	91.54(10)	O12−Er4−Se12	90.97(10)
Se11−Er4−Se12	89.22(2)	O11−Er4−Se12	77.97(11)
O10−Er4−Se10	87.49(10)	O12−Er4−Se10	89.74(10)
Se11−Er4−Se10	95.989(19)	O11−Er4−Se10	96.95(11)
C91−Se10−Er4	98.48(15)	Se12−Er4−Se10	174.73(2)
C103−Se12−Er4	100.23(17)	C97−Se11−Er4	97.21(16)

(42) Check, C. E.; Faust, T. O.; Bailey, J. M.; Wright, B. J.; Gilbert, T. M.; Sunderlin, I. S. *J. Phys. Chem. A* **2001**, *105*, 8111.

(43) Dunning, T. H.; Hay, P. J. In *Modern Theoretical Chemistry*; Schaefer, H. F., III, Ed.; Plenum: New York, 1976; Vol. *3*, pp 1−28.

(44) (a) Yang, J.; Dolg, M. *Theor. Chem. Acc.* **2005**, *113*, 212. (b) Weigand, A.; Cao, X.; Yang, J.; Dolg, M. *Theor. Chem. Acc.* **2009**, accepted. (c) Martin, J. M. L.; Sundermann, A. *J. Chem. Phys.* **2001**, *114*, 3408. MWB basis sets were retrieved from http://www.theochem.uni-stuttgart.de/pseudopotentials.

(45) (a) Dunning, T. H., Jr. *J. Chem. Phys.* **1989**, *90*, 1007. (b) Kendall, R. A.; Dunning, T. H., Jr.; Harrison, R. J. *J. Chem. Phys.* **1992**, *96*, 6796. (c) Woon, D. E.; Dunning, T. H., Jr. *J. Chem. Phys.* **1993**, *98*, 1358.

(46) (a) Reed, A. E.; Curtiss, L. A.; Weinhold, F. *Chem. Rev.* **1988**, *88*, 899. (b) Glendening, E. D.; Reed, A. E.; Carpenter, J. E.; Weinhold, F. *QCPE Bull.* **1990**, *10*, 58.

(47) Frisch, M. J.; et al. *Gaussian 03*, revision E.01; Gaussian, Inc.: Wallingford, CT, 2004. See the Supporting Information for the complete reference for Gaussian 03.

transmetalation reactions of elemental Yb with $Hg(SC_6F_5)_2$ in THF (eq 1),

$$2Yb + 3Hg(SC_6F_5)_2 \rightarrow 2(THF)_3Yb(SC_6F_5)_3 + 3Hg \quad (1)$$

whereas selenolate **2** can be prepared by the direct reduction of diselenide RSeSeR with elemental Er in THF (eq 2) and a trace Hg catalyst.

$$2Er + 3C_6F_5Se{-}SeC_6F_5 \rightarrow 2(THF)_3Er(SeC_6F_5)_3 \quad (2)$$

The different approaches reflect different chemistries associated with the ligands, not with the redox behavior of Ln, given that attempts to reduce the disulfide with both redox active and inactive Ln do not appear to proceed at an appreciable rate.

Both **1** and **2** adopt *mer*-octahedral geometries, with inequivalent chalcogenolate and THF ligand positions within the primary coordination sphere. In each structure, there is a consistent pattern of Ln−E bond lengths, with the Ln−E bond trans to anionic E significantly longer than the Ln−E bond trans to neutral THF. In thiolate **1**, there is a single crystallographically unique molecule in the unit cell, and the Yb−S2 bond [2.642(2) Å] trans to THF is 0.037 Å shorter than either of the Yb−S bonds [2.678(2) and 2.680(2) Å] trans to thiolate. The selenolate compound **2** shows the same directional dependence of the metal−ligand bond lengths, but in this case, there are four crystallographically independent molecules per unit cell and thus a range of bond-length differences. The Er−Se bonds trans to THF are 0.038 Å (Er1), 0.034 Å (Er2), 0.021 Å (Er3), and 0.029 Å (Er4) shorter than the average of the Er−Se bonds trans to SeC_6F_5. The bond-length difference in the thiolate compound is slightly greater (∼0.007 Å) than the average of the four sets of bond-length differences in the selenolate compound.

A similar pattern is noted for the Ln−O(THF) bonds; the Ln−O bond for the THF ligands trans to the chalcogenolate ligands is significantly longer than the Ln−O bonds trans to O(THF). In the thiolate compound **1**, the difference is 0.032 Å. In the selenolate compound **2**, the four independent molecules have Er−O bonds trans to Se that are 0.019 Å (Er1), 0.022 Å (Er2), 0.006 Å (Er3), and 0.030 Å (Er4) Å longer than the average of the Er−O bonds trans to THF. Again, the difference in the bond lengths is greater in the thiolate compound (by ∼0.013 Å). Attempts to measure the trans influence exerted by other Lewis bases invariably led to the formation of seven-coordinate species, either by incorporation of an additional base or by dative coordination of fluoride;[12,15,27] only the THF derivatives formed six-coordinate products.

The X-ray structure of **1** provided the initial geometry for unconstrained geometry optimizations of **1** and **2** carried out with several DFT calculations and ECP/basis set combinations (see the Computational Details section); no significant changes in the overall conformation occurred during any of the optimizations. The optimized PBE/BasisII Ln−E bond lengths are listed in Table 3 (full Cartesian geometries of **1** and **2** are available as Supporting Information). The computed metal−ligand bond lengths are systematically larger than the observed X-ray values, and the differences are largest for the weak Ln−O(THF) bonds. The computed Ln−O bond lengths, when O(THF) is trans to anionic E (Yb1−O2 and Er4−O11), deviate most strongly from the observed values (∼0.14 Å). Conversely, the corresponding computed Ln−E distances (Yb1−S2 and Er4−Se11) deviate less than 0.01 Å from the X-ray values. The distinct asymmetry observed in the metal−ligand bond lengths of **1** and **2** is clearly expressed, and even enhanced (relative to the crystallographic values), in the electronic structure calculations. We define the asymmetry parameter Δ_{Ln-E} as the difference between the Ln−E bond length, when trans to THF, and the average of the two Ln−E bond lengths, when trans to anionic E, and compute $\Delta_{Yb-S} = -0.060$ Å and $\Delta_{Er-Se} = -0.059$ Å, as compared with observed values of −0.037 and −0.029 Å (Er4), respectively. When Δ_{Ln-O} is defined in an analogous manner [Δ_{Ln-O} = (Ln−O bond length when trans to anionic E) − (average Ln−O bond length when trans to THF)], the computed asymmetry in Ln−O distances is also considerably larger than that observed, viz., $\Delta_{Yb-O} = \Delta_{Er-O} \sim 0.10$ Å, as compared with the experimental value of approximately 0.03 Å.

Computed values for the Ln−E bond lengths are not strongly sensitive to the type of DFT methodology used. Table S-1 in the Supporting Information presents optimized metal−ligand bond lengths for **1** and **2** obtained with BasisII and exchange-correlation functionals of increasing sophistication (representatives from different rungs on "Jacob's Ladder"[48]): PBE,[35] a pure generalized gradient approximation (GGA) functional (second rung; these data are also in Table 3); TPSS,[49] a meta-GGA functional (third rung); B3LYP,[50] the

Table 3. Comparison of Computed (PBE/BasisII) and Experimental (X-ray) Metal−Ligand Bond Lengths [Å] for **1** and **2**[a,b] and Computed (PBE/BasisII) Wiberg Bond Orders at DFT-Optimized and X-ray Geometries

	bond length		bond order	
	DFT	X-ray	DFT	X-ray
Yb1−O1	2.339	2.271	0.129	0.143
Yb1−O2	2.440	2.308	0.119	0.132
Yb1−O3	2.341	2.280	0.123	0.139
Yb1−S1	2.708	2.678	0.500	0.512
Yb1−S2	2.652	2.642	0.559	0.568
Yb1−S3	2.716	2.680	0.487	0.509
Δ_{Yb-O}[c]	0.100	0.033		
Δ_{Yb-S}[d]	−0.060	−0.037		
	bond length		bond order	
	DFT	X-ray	DFT	X-ray
Er4−O12	2.373	2.304	0.128	0.155
Er4−O11	2.478	2.337	0.114	0.142
Er4−O10	2.375	2.310	0.120	0.151
Er4−Se12	2.858	2.828	0.585	0.622
Er4−Se11	2.807	2.802	0.646	0.698
Er4−Se10	2.874	2.833	0.569	0.620
Δ_{Er-O}[c]	0.104	0.030		
Δ_{Er-Se}[d]	−0.059	−0.029		

[a] Cartesian geometries of **1** and **2** are available as Supporting Information. [b] Comparison is made to molecule 4 in the unit cell of **2** because the conformation of this molecule shows the strongest similarity to the conformation of **1**. [c] Δ_{Ln-O} = (Ln−O bond length when trans to anionic E) − (average Ln−O bond length when trans to THF). [d] Δ_{Ln-E} = (Ln−E bond length when trans to THF) − (average Ln−E bond length when trans to anionic E).

(48) Perdew, J. P.; Schmidt, K. In *Density Functional Theory and Its Applications to Materials*; Van Doren, V. E., Van Alsenoy, K., Geerlings, P., Eds.; American Institute of Physics Press: New York, 2001.

(49) Tao, J. M.; Perdew, J. P.; Staroverov, V. N.; Scuseria, G. E. *Phys. Rev. Lett.* **2003**, *91*, 146401.

(50) (a) Becke, A. D. *J. Chem. Phys.* **1993**, *98*, 5468. (b) Lee, C.; Yang, W.; Parr, R. G. *Phys. Rev. B* **1988**, *37*, 785.

standard hybrid-GGA functional (fourth rung); and, finally, M05,[51] representing hybrid meta-GGA functionals (also fourth rung). The bond lengths obtained with the TPSS, B3LYP, and M05 functionals are overall very similar in magnitude to those obtained with the PBE functionals; the largest differences in the stronger Ln−S,Se bonds are about 0.02 Å, whereas the differences in the weaker Ln−O bonds may approach 0.04 Å. With TPSS functionals, the Ln−O bonds are slightly shorter than those obtained with PBE, but the Ln−S,Se bonds are longer. The bond lengths obtained with the two hybrid functionals, B3LYP and M05, are mostly larger than those obtained with the functionals that do not contain exact exchange, PBE and TPSS. Importantly, substantial asymmetry in the metal−ligand bond lengths is present with all functionals applied. The asymmetry parameters (quoting data for **1** only; the results on **2** are similar) are larger for M05 ($\Delta_{Yb-S} = -0.062$ Å and $\Delta_{Yb-O} = 0.114$ Å) than for PBE ($\Delta_{Yb-S} = -0.060$ Å and $\Delta_{Yb-O} = 0.100$ Å) but slightly smaller for TPSS ($\Delta_{Yb-S} = -0.051$ Å and $\Delta_{Yb-O} = 0.075$ Å) and B3LYP ($\Delta_{Yb-S} = -0.063$ Å and $\Delta_{Yb-O} = 0.075$ Å).

Calculations with the smaller basis set (BasisI) and these same four DFT functionals (Table S-2 in the Supporting Information) generally result in slightly shorter bonds and diminished asymmetry parameters, relative to those obtained with BasisII. For example, the asymmetry parameters obtained for **1** using PBE functionals and BasisI are $\Delta_{Yb-S} = -0.048$ Å and $\Delta_{Yb-O} = 0.073$ Å. The additional calculations just summarized (variations in the applied DFT functionals and basis sets) support the conclusion that the computed bond lengths shown in Table 3, and the trends they display, are part of a general pattern and not fortuitous results arising from the selection of one particular computational model.

The computed charge distributions for **1** and **2** were subjected to NBO analysis.[46] Wiberg bond indices[52] for the metal−ligand bonds, obtained at the DFT equilibrium geometries and at the experimental X-ray geometries (PBE/BasisII), support the presence of covalent Ln−S,Se bonding (Table 3). At the DFT-optimized geometries, computed Yb−S bond orders are 0.49 and 0.50 for the two nearly equivalent Yb−S bonds but are larger at 0.56 for the Yb−S bond trans to THF. Similarly, the Er−Se bond orders for the nearly equivalent bonds are 0.64 and 0.66, whereas the unique Er−Se bond trans to THF shows a larger bond order of 0.69. The Ln−O bonds, on the other hand, are overwhelmingly ionic in character with uniformly small bond orders (∼0.12); the Ln−O bond order is smallest when the bond is trans to an anionic group. Within a particular type of bond (Yb−S, Er−Se, or Ln−O), the magnitude of the bond order correlates qualitatively with the length of the bond. The X-ray-derived geometries feature shorter metal−ligand bonds, and hence the bond orders obtained at these geometries are slightly larger than those at the computed equilibrium geometries (Table 3). However, the patterns exhibited by the bond orders are identical at the two sets of geometries. The distinctly nonzero Ln−E Wiberg bond orders support the notion that covalency contributes to Yb−S and Er−Se bonding; furthermore, the variations computed in these bond orders suggest that the asymmetry, computed and observed, in the length of the Ln−E bonds is associated with the differences in the magnitudes of the covalent interaction.

Table 4. Comparison of Computed (PBE/BasisI) Metal−Ligand Bond Lengths [Å] for **1** and **2** with Modified Yb or Er Basis Sets

Yb basis set	[5s4p3d]	[5s4p]	[5s4p2d][c]
Yb1−O1	2.331	2.399	2.389
Yb1−O2	2.411	2.410	2.429
Yb1−O3	2.344	2.383	2.400
Yb1−S1	2.727	2.877	2.806
Yb1−S2	2.681	2.867	2.780
Yb1−S3	2.729	2.874	2.797
Δ_{Yb-O}[a]	0.074	0.019	0.035
Δ_{Yb-S}[b]	−0.047	−0.008	−0.021

Yb basis set	[5s1p3d][d]	[2s4p3d]	[5s4p3d3f]	[5s4p3f]
Yb1−O1	2.322	2.288	2.322	2.372
Yb1−O2	2.388	2.391	2.405	2.397
Yb1−O3	2.337	2.318	2.335	2.374
Yb1−S1	2.717	2.727	2.719	2.864
Yb1−S2	2.675	2.677	2.674	2.850
Yb1−S3	2.720	2.732	2.719	2.860
Δ_{Yb-O}[a]	0.059	0.088	0.077	0.024
Δ_{Yb-S}[b]	−0.044	−0.052	−0.045	−0.012

Er basis set	[5s4p3d]	[5s4p]	[5s1p3d][c]	[2s4p3d]
Er4−O12	2.368	2.416	2.362	2.336
Er4−O11	2.443	2.440	2.419	2.414
Er4−O10	2.370	2.430	2.363	2.351
Er4−Se12	2.876	3.035	2.871	2.878
Er4−Se11	2.843	3.034	2.845	2.834
Er4−Se10	2.892	3.041	2.891	2.896
Δ_{Er-O}[a]	0.074	0.017	0.057	0.071
Δ_{Er-Se}[b]	−0.041	−0.004	−0.036	−0.053

[a] Δ_{Ln-O} = (Ln−O bond length when trans to anionic E) − (average Ln−O bond length when trans to THF). [b] Δ_{Ln-E} = (Ln−E bond length when trans to THF) − (average Ln−E bond length when trans to anionic E). [c] Innermost d-type basis function deleted. [d] Innermost p-type basis function kept.

As mentioned earlier, the electronic configuration for neutral Yb and Er considered in the calculations is formally $5s^25p^65d^16s^2$; hence, a metal electronic configuration approaching $5s^25p^65d^06s^0$ would be representative of a fully formed Ln^{III} cation. However, the natural electronic configurations (NECs) for Yb and Er in **1** and **2** are $5s^25p^{5.99}5d^{0.91}6s^{0.27}6d^{0.13}$ and $5s^25p^{5.98}5d^{1.16}6s^{0.29}6p^{0.01}6d^{0.13}$, respectively, resulting in formal charges of only 1.68+ for Yb and 1.41+ for Er. This analysis indicates that the positive charge on the Ln atom is associated exclusively with a loss of electron density from the 6s orbitals; Yb (or Er) actually has a slightly higher occupancy of d electrons in the valence shell in complex **1** (or **2**) than in the free atom. Virtually no changes occur in the Ln p orbital occupancies from the free atom to either complex. The low occupancy of metal 6s orbitals does not appear capable of inducing metal−ligand bond length asymmetry and, consequently, the NECs suggest that partial occupancy of d orbitals is the principal source of covalency and trans influence in Ln complexes **1** and **2**.

To further investigate this issue, additional geometry optimizations on complexes **1** and **2** were carried out with selectively modified Ln basis sets. Computed metal−ligand bond lengths from all of the calculations are available in Table S-3 in the Supporting Information; a condensed version is presented as Table 4. The Ln basis set in BasisI is of the [5s4p3d] type; i.e., there are three sets of d-type basis functions

(51) Zhao, Y.; Schultz, N. E.; Truhlar, D. G. *J. Chem. Phys.* **2005**, *123*, 161103.
(52) Wiberg, K. B. *Tetrahedron* **1968**, *24*, 1083.

covering the 5d (and higher) atomic orbitals, four p-type basis functions for the 5p (and higher) atomic orbitals, etc. This type of Yb basis set led to computed asymmetry parameters of $\Delta_{Yb-S} = -0.048$ Å and $\Delta_{Yb-O} = 0.073$ Å in **1** (Table 4 and Table S-3 in the Supporting Information). Upon deletion of the most diffuse d function from the Yb basis set, absolute changes in all Ln−E bond lengths are less than 10^{-3} Å and no changes occur to the asymmetry parameters. When the two outermost d functions are deleted, the Yb−S bonds lengthen by ∼0.01 Å and the Yb−O bonds shorten by ∼0.03 Å, resulting in small changes in the asymmetry parameters to $\Delta_{Yb-S} = -0.045$ Å and $\Delta_{Yb-O} = 0.061$ Å (Table S-3 in the Supporting Information). However, when all d-type functions are removed from the Yb basis set, all Ln−E bonds lengthen further as expected, but, importantly, the asymmetry in the Ln−E bonds essentially vanishes, $\Delta_{Yb-S} = -0.008$ Å and $\Delta_{Yb-O} = 0.019$ Å ([5s4p]; Table 4). Furthermore, it is the Yb−S bond situated trans to the THF molecule (Yb1−S2) that undergoes the largest change in the bond length and hence is most sensitive to the presence of d functions in the Yb basis set. Reduction of the 4p basis set to minimal size (to essentially just cover the $5p^6$ electrons), while keeping all of the d functions, induces only a small change in the asymmetry parameters (relative to their original values), $\Delta_{Yb-S} = -0.044$ Å and $\Delta_{Yb-O} = 0.059$ Å ([5s1p3d]; Table 4); hence, the more diffuse p functions do not appear to play a significant role in promoting the trans influence. As expected, removal of the two most diffuse s functions from the Yb basis set does not change the bond-length asymmetry parameters either (Table S-3 in the Supporting Information). However, if the s function that covers mostly 6s orbital space is also deleted, the asymmetry parameters actually increase ($\Delta_{Yb-S} = -0.052$ Å and $\Delta_{Yb-O} = 0.088$ Å); population of nondirectional metal s orbitals tends to diminish the asymmetry. When the basis set on Er is modified in **2**, the metal−ligand bond lengths change in similar patterns (Table 4). Whereas the initial asymmetry parameters were $\Delta_{Er-Se} = -0.041$ Å and $\Delta_{Er-O} = 0.074$ Å, deletion of all d-type basis functions on Er leads to a dramatic reduction to $\Delta_{Er-Se} = -0.004$ Å and $\Delta_{Er-O} = 0.017$ Å, but bringing the p-type basis set down to minimal size produces little change ($\Delta_{Er-Se} = -0.036$ Å and $\Delta_{Er-O} = 0.057$ Å). Furthermore, the addition of up to three sets of f-type polarization functions to the Yb basis set[44a] ([5s4p3d3f]) leads to a shrinkage of only ∼0.01 Å in all Ln−E bonds and virtually no change in the asymmetry parameters, $\Delta_{Yb-S} = -0.045$ Å and $\Delta_{Yb-O} = 0.077$ Å. On the other hand, substituting the f-type functions for the d-type functions ([5s4p3f] basis set) again removes most of the asymmetry ($\Delta_{Yb-S} = -0.012$ Å and $\Delta_{Yb-O} = 0.024$ Å).

Thus, the asymmetry in the metal−ligand bond lengths is brought about primarily by the presence of d-type basis functions in the Ln basis set. The magnitude of the asymmetry depends largely on the spatial extent of the innermost d-type function in the basis set, the one that corresponds most closely to what we commonly would refer to as the 5d orbital; deletion of just this single basis function from the Yb basis set leads to $\Delta_{Yb-S} = -0.021$ Å and $\Delta_{Yb-O} = 0.035$ Å ([5s4p2d]; Table 4). The calculations with modified Ln basis sets establish that it is primarily through Ln 5d orbitals that covalency and the trans influence are expressed in compounds **1** and **2**, substantiating the NEC results presented above.

Table 5. Summary of the Ln−Ligand Bond Lengths (Å) in Octahedral MX_3Y_3 Coordination Compounds

molecule	Ln−X trans to X	Ln−X trans to Y	Δ_{x-y}*[a]	ref
$(OPR_3)NdCl_3$	2.787(3)	2.709(3)	0.078	64
$(THF)_3YbCl_3$	2.532(3)	2.513(4)	0.019	55
$(THF)_3YbBr_3$	2.708(1)	2.665(1)	0.043	56
$(THF)_3YbI_3$	2.954(2)	2.915(2)	0.039	57
$(HMPA)_3PrCl_3$	2.729(3)	2.706(3)	0.023	63
$(HMPA)_3DyCl_3$	2.636(3)	2.626(4)	0.010	65
$(HMPA)_3YbCl_3$	2.591(4)	2.582(5)	0.009	66
$(py)_3Yb(SPh)_3$	2.666(2)	2.609(4)	0.057	12
$(py)_2(THF)Sm(SR)_3$	2.750(3)	2.720(3)	0.030	53
$(HMPA)_3Sm(SPh)_3$	2.826(2)	2.811(1)	0.015	67
$(HMPA)_3Yb(SPh)_3$	2.734(1)	2.718(1)	0.016	67
$(THF)_3Yb(OC_6F_5)_3$	2.111(2)	2.084(2)	0.027	15
$(THF)_3Yb(SC_6F_5)_3$	2.679(2)	2.642(2)	0.039	this work
$(THF)_3Er(SeC_6F_5)_3$	2.836(2)	2.805(2)	0.031	this work

[a] Δ_{x-y}* = (average Ln−X trans to X) − (average Ln−X trans to Y), where X is the anionic ligand and Y is the neutral donor ligand. If there is more than one crystallographically independent molecule/cell, the average distances for all of the molecules in the cell are used.

Discussion

Both **1** and **2** have directionally dependent Ln−ligand bond lengths, with Ln−ligand bonds trans to anions that are consistently longer than the same Ln−ligand bonds that are trans to neutral donor ligands. While this concept of a trans influence is well established in transition-metal and main-group chemistry, until now there has never, to our knowledge, been an experimental−theoretical investigation into the possibility of Ln molecules showing the same effect.

These bond-length distributions have been measured frequently, but noted rarely, for a wide range of *mer*-octahedral LnX_3Y_3 (X = anion and Y = neutral donor) coordination complexes. Table 5 contains a list of Ln−X bond lengths for the known *mer*-LnX_3Y_3 compounds that have been characterized by X-ray diffraction. In every case, anions trans to anions are further from Ln than are anions trans to neutral donors. The same effect is also noted in cubane cluster derivatives and a group of octahedral LnX_4Y_2 coordination compounds. Table 6 shows the range of Ln compounds with octahedral coordination environments and their associated trans influences, ranging from charge-neutral cesium(IV) alkoxides to anionic $(DME)Yb(SePh)_4^-$. Again, in every case, there is a directional component to the bonding, with bonds trans to anions significantly longer than bonds trans to neutral donor ligands. The trans influence appears to be a general, fundamental property of Ln coordination compounds.

Both electropositive (i.e., SePh) and electronegative (i.e., OC_6F_5) ligands display a trans influence. The directionality was first noted in the description of $(py)_3Yb(SPh)_3$,[12]

(53) Mashima, K.; Nakayama, Y.; Fukumoto, H.; Kanehisa, N.; Kai, Y.; Nakamura, A. *J. Chem. Soc., Chem. Commun.* **1994**, 2523.
(54) (a) Shotwell, J. B.; Sealy, J. M.; Flowers, R. A. *J. Org. Chem.* **1999**, *64*, 5251. (b) Kramer, G. M.; Mass, E. T.; Dines, M. B. *Inorg. Chem.* **1980**, *20*, 1415. (c) Kramer, G. M.; Mass, E. T.; Dines, M. B. *Inorg. Chem.* **1980**, *20*, 1418.
(55) (a) Deacon, G. B.; Feng, T.; Junk, P. C.; Skelton, B. W.; Sobolev, A. N.; White, A. H. *Aust. J. Chem.* **1998**, *51*, 75. (b) Qian, C.; Wang, B.; Deng, D.; Xu, C.; Sun, X.; Ling, R. *Jiegou Huaxue* **1993**, *12*, 18.
(56) Deacon, G. B.; Feng, T.; Junk, P. C.; Meyer, G.; Scott, N. M.; Skelton, B. W.; White, A. H. *Aust. J. Chem.* **2000**, *53*, 853.
(57) Emge, T. J.; Kornienko, A.; Brennan, J. G. *Acta Crystallogr.* **2009**, *C65*, m422.

Table 6. Summary of the Ln−Ligand Bond Lengths (Å) in Octahedral Compounds

	Ln−X trans to X	Ln−X trans to Y	Δ_{x-y}*[a]	ref
[(BIPY)Yb(SBu)$_3$]$_2$	2.627(3)	2.620(3)	0.007	68
Ce(OR)$_4$(4-NMe$_2$py)$_2$	2.127(3)	2.112(5)	0.015	69
Ce(hfip)$_4$(TMEDA)	2.152(6)	2.115(5)	0.037	70
(DME)Yb(SePh)$_4^-$	2.791(2)	2.781(2)	0.010	71
Sm$_2$I$_4$(N-MeIm)$_4$	3.307(1)	3.280(1)	0.027	72
(py)$_8$Yb$_4$Se$_4$(SePh)$_4$	2.803(2)	2.770(2)	0.033	13[b]
(py)$_{10}$Yb$_6$S$_6$(SPh)$_6$	2.669(6)	2.646(6)	0.023	13[c]
(THF)$_{10}$Yb$_6$Se$_6$I$_6$	2.785(2)	2.742(2)	0.037	14[d]

[a] Δ_{x-y}* = (average Ln−X trans to X) − (average Ln−X trans to Y), where X is the anionic ligand and Y is the neutral donor ligand. If there is more than one crystallographically independent molecule/cell, the average distances for all of the molecules in the cell are used. [b] Yb−μ_3Se^{2-} bonds trans to SePh or py. [c] Yb−μ_3S^{2-} bonds trans to SPh or py. [d] Yb−μ_3Se^{2-} bonds trans to I or THF.

where it was pointed out that the related compound (py)$_3$Sm(SC$_6$H$_3$^{i}Pr$_3$)$_3$[53] had a similar range of geometry-dependent Ln−S bond lengths. Subsequent studies on the NIR emission behavior of Ln(OC$_6$F$_5$)$_3$ revealed that (THF)$_3$-Yb(OC$_6$F$_5$)$_3$[15] displayed equally distinctive bond-length patterns. This phenoxide compound was actually the inspiration for the present work, because while the initial cursory examination of the bond lengths revealed the expected pattern, a closer examination of the structure suggested that interligand $\pi-\pi$ interactions were also capable of distorting Ln−X bond lengths to a similar degree.

Compounds **1** and **2** were subsequently targeted in an attempt to evaluate the various steric and electronic factors that might be important in influencing the bond lengths, but given the broad range of differences in the Er−Se and Er−O bond lengths for the four crystallographically independent molecules in **2**, it is clearly impossible to confidently separate contributions from lattice/steric/electronic influences or to state unequivocally that one ligand has a stronger covalent trans influence than does another. This is also similar to findings in main-group and transition-metal systems,[11] where it has been noted that intermolecular interactions are often greater than, or equal to, the effect that a trans influence might have on a bond length.

There are, however, a number of trends in the available data. First, it appears that the basicity of the neutral donor ligand has a measurable impact on the bond length trans to it. There are two molecular pairs in Table 5 with different neutral donors: (L)$_3$Sm(SPh)$_3$ (L = HMPA, py/THF) and L$_3$Yb(SPh)$_3$ (L = HMPA, pyridine). In both cases, the compound with the neutral donor that is the strongest donor ligand[54] also has the greater trans influence.

Second, the differences in the Ln−X bond lengths are significantly greater when steric interactions are minimal, i.e., in the first half of the Ln series. Of the five chloride structures listed in Table 5, the two with the greatest trans influence are Pr and Nd compounds. This can be rationalized by noting that for six-coordinate structures the larger Ln compounds are impacted less by steric repulsions that might tend to overshadow any trans influence, but it does run contrary to the assumption that any sort of metal−ligand orbital overlap will increase as the d orbitals contract across the Ln series. Alternatively, it could be argued that the early Ln−X bonds are weaker and thus more susceptible to a trans influence.

Third, there is no fixed period for which trans influences are maximum. For the set of (THF)$_3$Ln(EC$_6$F$_5$)$_3$ (E = O, S, Se), the effect is at a maximum value for S, with S > Se > O, and in the halide derivatives (THF)$_3$LnX$_3$ (X = Cl,[55] Br,[56] I[57]), there is a maximum value for Br, with Br > I > Cl . This is not surprising, given that any trans influence reflects both the ability of an ion to donate electron density and the ease with which a given ion−metal bond can be distorted. While it is tempting to note that most, but not all, of the largest trans influences are found in compounds that contain more covalent/less electronegative ligands, these are also the least stable complexes with the longest M−L bond lengths under consideration, and as such, these contain the bonds that should be distorted most easily.

Bonds between Ln and the neutral donors also tend to follow the same bond-length distribution patterns, with bonds trans to anions longer than bonds trans to neutral donors. In **1**, the Yb−O bonds trans to O are 2.271(4) and 2.280(4) Å, and the Yb−O bond trans to S is significantly longer, at 2.308(5) Å. A similar pattern is noted for the four independent molecules in **2**, but the differences change significantly within the independent molecules. Because these dative interactions are significantly weaker than bonds between charged species, they should be particularly susceptible to influences such as crystal-packing effects. An example of this behavior was noted in the structures of [(DME)$_3$-Ln(SC$_6$F$_5$)$_2$]$^+$ (Ln = La−Gd), where Ln−anion bond lengths varied consistently with the Ln ionic radius, while the dative Ln−F separations initially followed the expected trend but then increased with decreasing Ln as ligand−ligand repulsions increased.[58] For this reason, we have chosen not to focus attention on variations in the bond lengths between Ln and neutral donor ligands, even though the measured distances in **1** and **2** are consistent with theoretical predictions (cf. Table 3).

Fluorination of the arene group appears to increase the length of the Ln−Se bond and decrease the length of the Er−O(THF) bond, which is consistent with an electrostatic component to the bonding, because the polarizing influence of the electronegative F atoms lessen the charge density at the Se atom. The average Er−Se bond length in the *fac*-octahedral selenolate (THF)$_3$Er(SePh)$_3$ is significantly shorter, at 2.7766(6) Å, than either the average (for the four independent molecules) of the crystallographically unique Er−Se bond trans to THF in **2** [2.8042(7) Å] or the average of all of the Er−Se bonds in **2** (2.8256 Å). Given trans influences, the former comparison seems more appropriate. In contrast, the average Er−O(THF) distances for **2** (2.304 Å) are significantly shorter than the three crystallographically equivalent Er−O(THF) bonds in (THF)$_3$Er(SePh)$_3$ [2.347(3) Å].[59] This is again consistent with an electrostatic bonding model, in which fluorination of the selenolate withdraws the electron density from the Er^{III} ion, which then compensates by bonding more strongly with the THF ligands. A similar effect was noted in comparisons between Ln−SC$_6$F$_5$ and Ln−SC$_6$H$_5$ compounds.[60]

While a trans influence is noted here, Ln chemistry is still best described in ionic terms, and this is evident from the data

(58) Banerjee, S.; Emge, T. J.; Brennan, J. G. *Inorg. Chem.* **2004**, *43*, 6307.
(59) Lee, J.; Freedman, D.; Melman, J. H.; Brewer, M.; Sun, L.; Emge, T. J.; Long, F. H.; Brennan, J. G. *Inorg. Chem.* **1998**, *37*, 2512.
(60) Melman, J.; Rhode, C.; Emge, T. J.; Brennan, J. G. *Inorg. Chem.* **2002**, *41*, 28.

in Tables 5 and 6. In particular, the uniformity of the trans influence can be interpreted as an artifact of predominantly ionic behavior. In every Ln compound, the negatively charged ligand lengthens the bond trans to it and thus has the stronger trans influence, whereas in transition-metal systems, trans influences occur but relative bond lengthening can be found trans to either anions or neutral donors. Compare, for example, $GaCl_3(terpy)$,[61] where the Ga−Cl bond trans to N is 0.13 Å *shorter* than the average of the Ga−Cl bonds trans to Cl, with $IrCl_3(PMe_2Ph)_3$,[62] where Cl trans to P is 0.084 Å *longer* than the Ir−Cl bonds trans to Cl. It would be interesting to determine the structure of a LnX_3Y_3 compound with a phosphine donor ligand.

The magnitudes of the trans influences also reflect the essentially ionic character of the Ln−X bond. The range of bond-length differences noted in these Ln compounds is significantly smaller than the range of trans influence found in main-group or transition-metal structures,[11] even though the Ln−X bonds are considerably longer. This would be consistent with a greater covalent character for the latter metals relative to the Ln compounds.

Conclusion

Covalent bonding can have a measurable impact on the structures of Ln coordination complexes. DFT calculations indicate that the inequivalent bond lengths found in octahedral Ln coordination complexes result from a covalent bonding interaction between ligand-based p orbitals and the Ln 5d orbitals. Arguably, the present work is the first combined experimental−theoretical investigation demonstrating that covalent bonding is responsible for the directionality noted in Ln−X bond lengths.

Acknowledgment. We acknowledge support of the NSF (Grant CHE-0747165). We thank anonymous reviewers for constructive comments.

Supporting Information Available: X-ray crystallographic files in CIF format for the crystal structures of **1** and **2**; complete ref 47, optimized geometries of **1** and **2**, Tables S-1−S-3, and a summary of the crystallographic details. This material is available free of charge via the Internet at http://pubs.acs.org.

(61) Beran, G.; Carty, A. J.; Patel, H. A.; Palenik, G. J. *Chem. Commun.* **1970**, 222.
(62) Aslanov, A.; Mason, R.; Wheeler, A. G.; Whimp, P. O. *Chem. Commun.* **1970**, 30.
(63) Spichal, Z.; Necas, M.; Pinkas, J. *Inorg. Chem.* **2005**, *44*, 2074.
(64) Radonovich, L. J.; Glick, M. D. *J. Inorg. Nucl. Chem.* **1973**, *35*, 2745.
(65) Xing-Wang, Z.; Xing-Wang, L.; Benetollo, F.; Bombieri, G. *Inorg. Chim. Acta* **1987**, *139*, 103.
(66) Hou, Z.; Kobayashi, K.; Yamakazi, H. *Chem. Lett.* **1991**, 265.
(67) Mashima, K.; Nakayama, Y.; Shibahara, T.; Fukumoto, H.; Nakamura, A. *Inorg. Chem.* **1996**, *35*, 93.
(68) Aspinall, H. C.; Cunningham, S. A.; Maestro, P.; Macaudiere, P. *Inorg. Chem.* **1998**, *37*, 5396.
(69) Suh, S.; Guan, J.; Miinea, L. A.; Lehn, J. S.; Hoffman, D. M. *Chem. Mater.* **2004**, *16*, 1667.
(70) Evans, W. J.; Rabe, G. W.; Ziller, J. W. *Inorg. Chem.* **1994**, *33*, 3072.
(71) Geissinger, M.; Magull, J. *Z. Anorg. Allg. Chem.* **1995**, *621*, 2043.
(72) Daniele, S.; Hubert-Pfalzgraf, L. G.; Perrin, M. *Polyhedron* **2002**, *21*, 1985.